1993년도 한국음향학회 학술논문발표회 논문집(제 12권 1(s)호)

압전소자상의 탄성표면파 전파특성

노용래, 배영호, 정대식
산업과학기술연구소

SAW Propagation Properties on Piezoelectric Materials

Yongrae Roh, Youngho Bae and Daesik Chung
Research Institute of Industrial Science and Technology

1. Introduction

There are a number of piezoelectric materials available to the SAW component designer; the choice depends on the type of the device to be prepared, the frequency of operation, the bandwidth, the time delay, and the system use. In this study, characteristics of a piezoelectric material are evaluated for its various crystal cuts and directions to pick up the optimum orientation for the use as a substrate of a SAW device. Our specific application is SAW chemical sensors. The single crystal $LiTaO_3$ is chosen for the substrate material due to its high coupling factor, low temperature coefficient, and easy availability. Of the many criteria for evaluation, eight main items are selected such as the velocity, the coupling factor, the surface permittivity, the frequency-temperature coefficient, the air loading attenuation, the pure mode propagation, the beam steering and the misalignment sensitivity. Analysis of the results reveals the optimum orientation meet ing our requirements.

2. Numerical Calculation

Material properties of the $LiTaO_3$ are cited from Ref. 1. We apply the eight criteria in Sec. 1 to a variety of cuts and axes of the wafer to pick up the optimum orientation. Each criterion and corresponding calculation method is described as follows. Results are displayed for a representative case, i.e., Y-cut plane.

2.1. SAW Velocity

Unless the velocity difference for different orientations is very large, the absolute velocity should not be a major condition to choose a material. Figure 1 shows variation of the velocity with propagation directions on the Y-cut plane. Denoted values are unstiffened velocity (v_0). Similar results can be displayed for the stiffened velocity v_∞. For our purpose, the direction of high velocity is desirable, which leads to the selection of the Z axis on the plane.

2.2. Electromechanical Coupling Factor

The electromechanical coupling constant k^2 is related to the fractional change in SAW velocity when a thin, massless conductor is deposited on the propagation surface [2] as noted in

$$k^2 = 2\left(1 + \varepsilon_0/\varepsilon_p^T\right)\Delta v / v_\infty\left(1 - \Delta v / v_\infty\right) \qquad (1)$$

where Δv is $v_0 - v_\infty$, ε_0 is the dielectric constant of free space and

$$\varepsilon_p^T = \left(\varepsilon_{11}^T \varepsilon_{33}^T - \varepsilon_{13}^{T\,2}\right)^{1/2} \qquad (2)$$

ε_p^T is named the surface permittivity of the substrate. The ε_{ij}^T are the dielectric constants of the piezoelectric substrate. The superscript T means measurement at constant stress. Figure 2 shows the results evaluated on the Y-cut plane. Strong piezoelectric coupling is desirable for our purpose and, hence, the Z axis is the best.

2.3. Surface Permittivity

Following Ingebrigtsen [3], in the quasi-static approximation, the potential ϕ and power P of the surface wave is inversely proportional to ε_p^T. Large ϕ and P corresponds to small ε_p^T. ε_p^T is also involved in the coupling factor k^2. However, ε_p^T is usually almost constant for

various cuts and directions of a given crystal. Hence it must be a secondary factor to be considered.

2.4. Frequency -Temperature Coefficient (FTC)

It is desirable for a particular cut and crystal axis to have an almost negligible temperature coefficient concerning SAW propagation. For each point to be tabulated, we fix a reference temperature (25°C) and calculate the phase velocity at another temperature T + ΔT where ΔT is set 25°C. The velocity at 25°C has been already determined in Sec. 2.1. With the two phase velocities, FTC is obtained as

$$FTC = \frac{\Delta V}{\Delta T\, V_{01}} * 10^6 \ (ppm) \qquad (3)$$

where ΔV is V_{01} - V_{02}, V_{01} and V_{02} are the two velocities. Variation of the FTC on the Y-cut plane is described by Fig. 3. Z axis and 60° rotated Z axis are preferred.

2.5. Air Loading Attenuation

According to Artz [4], the attenuation coefficient α due to gas loading can be expressed in the following form.

$$\alpha = \rho_g V_g / \rho_s V_s \lambda_s \ (\text{Nepers / m}) \qquad (4)$$

where ρ_g is the density of the gas, V_g is the longitudinal wave velocity in the gas, ρ_s is the density of the surface wave substrate, V_s is the Rayleigh wave velocity, and λ_s is the Rayleigh wave wavelength. Center frequency of the SAW is assumed to be 1 MHz. Figure 4 shows calculation results on the Y-cut plane with air loading where ρ_g is 1.29 kg/m^3 and V_g is 340 m/s.

2.6. Pure Mode Propagation

In pure mode directions, the Rayleigh wave is not coupled with other types of SAWs. Some workers confuse pure mode propagation with no beam steering propagation. We differentiate one from the other in that the direction of no beam steering does not guarantee that uncoupling. To be pure mode, in the secular equation of the SAW [6], we should have null values for the elastic stiffness constant $C_0 = C_{14}^2 + C_{16}^2 + C_{34}^2 + C_{36}^2 + C_{45}^2 + C_{56}^2$ as well as the piezoelectric constant $e_0 = e_{14}^2 + e_{16}^2 + e_{34}^2 + e_{36}^2$. Figure 5 shows the variation of the C_0 and a similar graph can be drawn with the e_0. Z axis is the only pure mode direction.

2.7. Beam Steering

In the near field of each IDT, the disturbance propagates with no distortion, but the radiation makes an angle γ with the x axis, normal to the wavefronts. The angle γ is called the beam steering angle, and generally depends on the orientation angle θ with respect to a given crystal axis as

$$\text{Tan}\,\gamma = \frac{1}{v_0}\frac{dv_0}{d\theta} \qquad (5)$$

The smaller is the γ, the better is the device performance. From figure 6, Z axis and every 45° rotated direction from the Z axis are fine.

2.8. Misalignment Sensitivity

In the case γ is zero, however, beam steering can still arise in practice because of an error in the angle θ due to misalignment of an IDT. For small errors, γ can be found from the equation given by

$$\frac{d\gamma}{d\theta} = \frac{1}{v_0}\frac{d^2 v_0}{d\theta^2}\text{Cos}^2\gamma - \text{Sin}^2\gamma \qquad (6)$$

that is defined misalignment sensitivity. In principle, the misalignment error should be a secondary factor because every possible method is usually taken to preserve precise alignment.

For selection of the optimal orientation, the whole effects of the above eight criteria should be analyzed with a certain scheme of priority. Once the scheme is set up, the calculation is performed for various cuts and directions of the $LiTaO_3$ substrate. Table 1 illustrates the results for primary crystal symmetry. Our use of a SAW sensor requires such primary factors as (1) pure mode propagation (i.e., $C_0 = e_0 = 0$), (2) the maximum coupling factor, (3) the minimum FTC, (4) the minimum air loading attenuation, and (5) no beam steering angle. Secondary considerations include (1) the maximum velocity, (2) the minimum surface permittivity, and (3) the minimum misalignment sensitivity. In this sense, the optimum orientation is determined to be the Y-cut and Z-axis.

3. Conclusion

Characteristics of a piezoelectric single crystal $LiTaO_3$ are evaluated to determine the optimal surface orientation for use as a SAW device substrate. Theoretical calculations reveal that Y-cut and Z-axis is the optimal SAW propagation path.

References

1. K. H. H. O. Modelung, Numerical data and functional relationships in science and technology, Springer-Verlag, New York, 1984

2. M. B. Schulz and J. H. Matsinger, Applied Physics Letters, vol. 22, pp. 367-369

3. K. A. Ingebrigtsen, Journal of Applied Physics, vol. 40, pp. 2681-2686, 1969

4. R. M. Artz, E. Salzmann, K. Dransfeld, Applied Physics Letter, vol. 10, p. 165, 1967

5. V. V. Varadan, Y. R. Roh and V. J. Varadan, Proceedings of Ultrasonics Symposium, pp. 591-594, 1989

6. T. L. Szabo and A. J. Slobodnik, Jr., IEEE Transactions on SU, Vol. 20, pp. 240-251, Jul. 1973

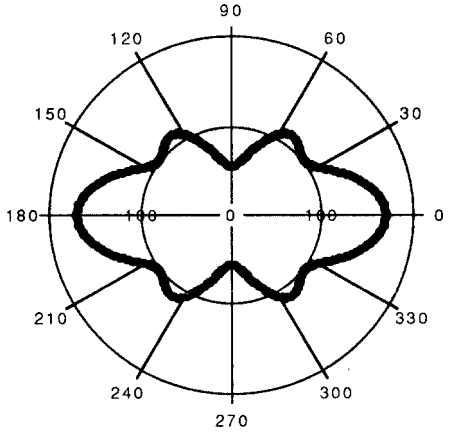

Fig. 1. Variation of unstiffened Rayleigh wave velocity on the Y-cut plane. Angle θ is the crystal Z-axis and numbers on the circumference means that much rotation in degrees from the Z-axis. Numbers on the radius added with 3100 are absolute velocity of the wave.

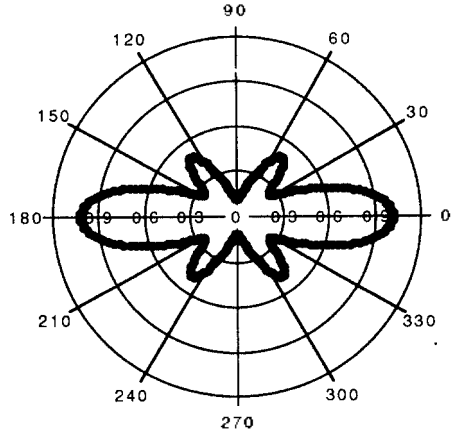

Fig. 2. Variation of the coupling factor on the Y-cut plane. Numbers on the radius are absolute values of the factor in percent.

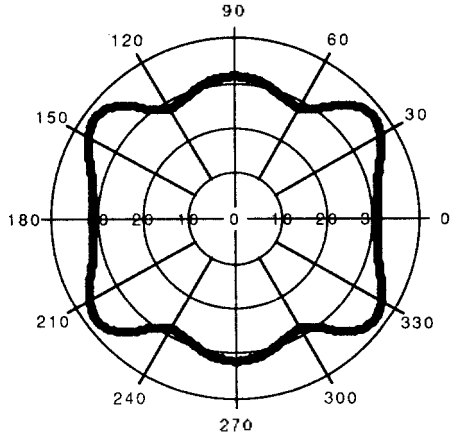

Fig. 3. Variation of the FTC on the Y-cut plane. Numbers on the radius are absolute values of the FTC in ppm.

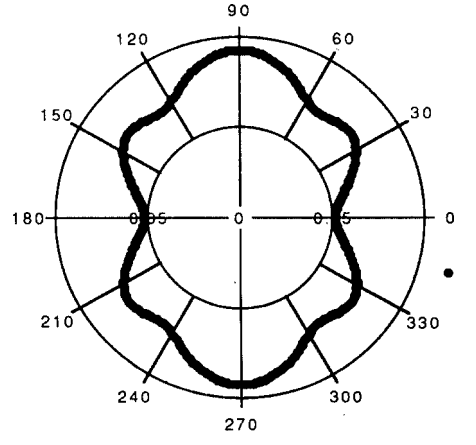

Fig. 4. Variation of the attenuation coefficient a on the Y-cut plane. Numbers on the radius are absolute values of the a in Nepers.

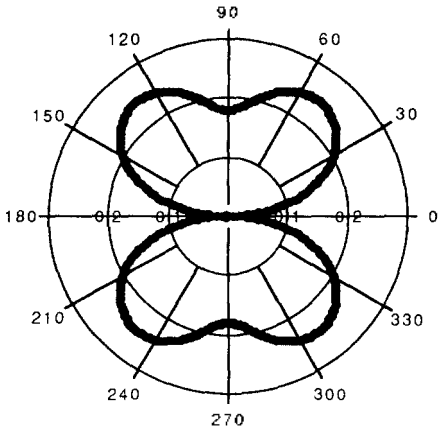

Fig. 5. Variation of the C_0 on the Y-cut plane. Absolute value of C_0 has no meaning.

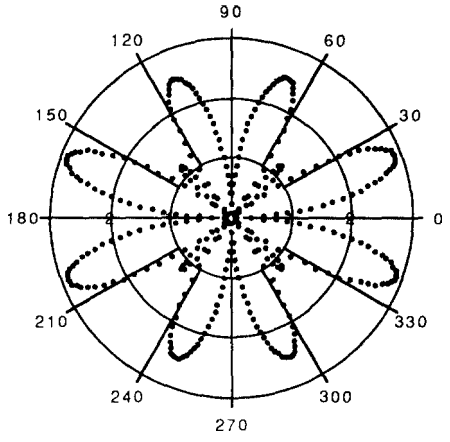

Fig. 6. Variation of the beam steering angle γ on the Y-cut plane. Numbers on the radius are absolute values of the γ in degrees.

Table 1. Calculation results of the eight items for representative symmetric orientations of $LiTaO_3$

cut	prop. direction *priority*	$C_0 + e_0$ *1*	k2 (%) *2*	FTC (ppm) *3*	α *4*	γ *5*	V_0 *6*	$\varepsilon_p^T / \varepsilon_0$ *7*	misalign. sen. *8*
Z cut	X axis	1.817	0.107	50.00	0.566	0.0	3229	42.75	0.406
	30 rotated X axis	0.000	0.796	52.47	0.529	0.0	3340	42.71	1.090
	60 rotated X axis	1.817	0.107	50.00	0.566	0.0	3229	42.64	0.406
	90 rotated X axis	0.000	0.796	52.47	0.529	0.0	3341	42.60	1.090
167 Z cut	Y axis	0.000	0.337	56.31	0.562	0.0	3241	42.75	0.501
	67 rotated Y axis	1.011	1.047	49.05	0.517	0.0	3378	42.74	1.101
	90 rotated Y axis	0.522	0.293	51.45	0.546	0.0	3287	42.74	0.558
Y cut	Z axis	0.000	1.021	30.81	0.552	0.0	3270	43.75	0.210
	58 rotated Z axis	3.080	0.448	28.55	0.573	0.0	3208	43.64	0.245
	90 rotated Z axis	4.026	0.119	31.60	0.593	0.0	3155	42.60	0.162
36 Y cut	X axis	2.387	0.293	32.92	0.544	0.0	3294	42.65	0.371
	27 rotated X axis	0.000	1.070	26.22	0.537	0.0	3315	43.67	0.357
	90 rotated X axis	2.977	0.408	40.12	0.573	0.0	3208	42.75	0.330
X cut	138 rotated Y axis	3.335	0.011	41.92	0.602	0.0	3132	42.67	0.121